

# Temperature Dependence of the STIS CCD Dark Rate During Side-2 Operations

---

Thomas M. Brown  
October 5, 2001

---

## ABSTRACT

*Due to a failure of the primary (Side-1) STIS electronics, the STIS has been operating on its redundant (Side-2) electronics since July 2001. Side 2 does not have a functioning temperature sensor for the CCD, and so a constant current is applied to the CCD thermoelectric cooler. Thus, Side-2 operations exhibit a variation in CCD temperature that was not present during Side-1 operations. Fortunately, these variations in temperature can be tracked by a temperature sensor on the CCD housing. In this report, I describe the temperature dependence of the STIS CCD dark rate. For pixels at a given dark rate, the change in rate with temperature is extremely linear over the observed range in CCD housing temperature (approximately 3 °C). However, the change in rate with temperature depends upon the rate itself. Pixels with very low dark rates ( $\ll 0.01 e^- s^{-1}$ ) show a 4%/°C rate variation; moderately hot pixels ( $0.1 e^- s^{-1}$ ) show a 8%/°C rate variation, while the hottest pixels ( $> 1 e^- s^{-1}$ ) show a 6%/°C rate variation.*

---

## Introduction

On 16 May 2001, the primary (Side-1) set of STIS electronics failed, and operations were subsequently resumed on the redundant (Side-2) set. Although most operations on Side 2 are identical to those on Side 1, some of the thermal control of the STIS CCD has been lost. On Side 1, a temperature sensor mounted on the CCD carrier provided closed-loop control of the current provided to the thermoelectric cooler (TEC), thus ensuring a

stable detector temperature at the commanded set point ( $-83\text{ }^{\circ}\text{C}$ ). Side 2 does not have a functioning temperature sensor, and so the TEC is run at a constant current. Thus, under Side-2 operations, the CCD temperature varies with that of the spacecraft environment, and these temperature changes are accompanied by changes in detector dark rate. Because the current to the TEC is now fixed at a higher value than the typical value required to hold the  $-83\text{ }^{\circ}\text{C}$  set point on Side 1 (i.e., 3 A vs. 2.7 A), the detector is often cooler than it was during Side-1 operations. The result is that the median dark rate varies from 4 to 5  $\text{e}^{-}$  per 1000 s on Side 2, as opposed to 4.6 to 5  $\text{e}^{-}$  per 1000 s on Side 1.

Using data from dark rate monitoring programs, I have characterized the dark rate dependence on the CCD housing temperature. Although no sensor is available to measure the temperature of the CCD itself, there is a sensor for the CCD housing temperature, associated with telemetry keyword OCCDHT. The hot side of the TEC is bonded to the CCD housing baseplate; hence with fixed TEC current, the CCD housing should track closely the detector temperature under Side-2 operations, and this can be seen by the excellent correlation between the dark rate and the housing temperature (reported in the following sections). Note that the CCD housing is far hotter than the detector itself: the housing temperature is approximately  $18\text{ }^{\circ}\text{C}$  during normal operations, while the detector runs at approximately  $-83\text{ }^{\circ}\text{C}$ .

## Data Reduction

The analysis focused on approximately 2 months of data from programs 8864 and 8901, spanning the time period from 13 July 2001 to 21 September 2001. I used the long exposures (1100 s each) from these programs, taken with a gain of 1 and no on-orbit binning. At the time of this writing, there have been three CCD anneals since the start of Side-2 operations. During each anneal, the TEC is turned off, and the rise in CCD temperature repairs some of the hot pixels that have accumulated in the detector. Thus, I grouped these data into 3 subgroups, representing each period between anneals.

The raw frames were processed through the CALSTIS pipeline, which includes a bias subtraction from the CCD overscan region and the subtraction of a superbias. A mean temperature for each frame was calculated by averaging the CCD housing temperature, as a function of time, across the time period spanned by the exposure. The processed frames in each anneal period were then sorted by temperature. Groups of 3 frames, with each frame having nearly the same temperature, were combined with cosmic-ray rejection, using the OCCREJECT routine. Each resulting coadded frame was assigned a new temperature, from the mean of its three input frames.

## Analysis

For the data in each anneal period, I designated the two frames closest to 18 °C as reference frames, hereafter referred to as RF1 and RF2. The temperature in each anneal period randomly varied from approximately 15.5 °C to 20 °C, with frames often near 18 °C, so this temperature makes a good reference point in the middle of the range. Then, I divided the frames in a given anneal period by RF1, and plotted the result versus RF2\* ; this was done for all frames in each anneal period, except for RF1 and RF2 themselves. An example of such a ratio is shown in Figure 1, which shows the change in dark rate for a 1.77 °C temperature change, plotted as a function of dark rate for each pixel. The curve shows the median ratio at each point along the x-axis. The horizontal line is simply the median of the curve, and the difference between the curve and line shows that the rate in an entire dark frame does not simply scale with temperature.

Once this was done for all of the frames in a given anneal period, the data from all anneal periods were combined, and I calculated the change in rate with temperature for given ranges in rate. The result is shown in Figure 2. For pixels with any given dark rate, the change in rate with temperature is very linear, and the fitted relations show very little scatter. However, as was already evident from Figure 1, the slope of this relation is a function of the rate itself. Figure 3 shows the fractional change in dark rate with temperature, as a function of rate.

It should be noted that the unnormalized dark rates do show some variation when comparing different anneal periods. At any given temperature, the median of a dark frame in the third anneal period was nearly 10% higher than that in the first two anneal periods. However, the dark rate variation with temperature within the third anneal period was the same as the first two anneal periods, and this is why the normalized data, shown in Figures 2 and 3, show little scatter.

\* Although it is a digression, the need for two reference frames near 18 °C may not be immediately obvious, so I will briefly explain. The use of two reference frames makes the abscissa and ordinate independent of one another. If one simply defines a single reference frame at a given temperature, RF1, and plots the ratio of a given dark frame to RF1 versus the rate in RF1 itself, the resulting function will be skewed. I show this in Figures 4 and 5. Figure 4 correctly uses two reference frames, and shows the ratio of an 18.25 °C frame to an 18.05 °C frame, against the rate in a 17.95 °C frame. The median ratio at any given rate is nearly unity - the curve and line are almost indistinguishable, as expected from the small change in temperature. In Figure 5, I incorrectly use only one reference frame, and plot the ratio of an 18.25 °C frame to an 18.05 °C frame, against the same 18.05 °C frame. The curve is now dominated by the fact that the ordinate and abscissa are not independent, with the distribution at the low count-rate end driven by Poisson statistics.

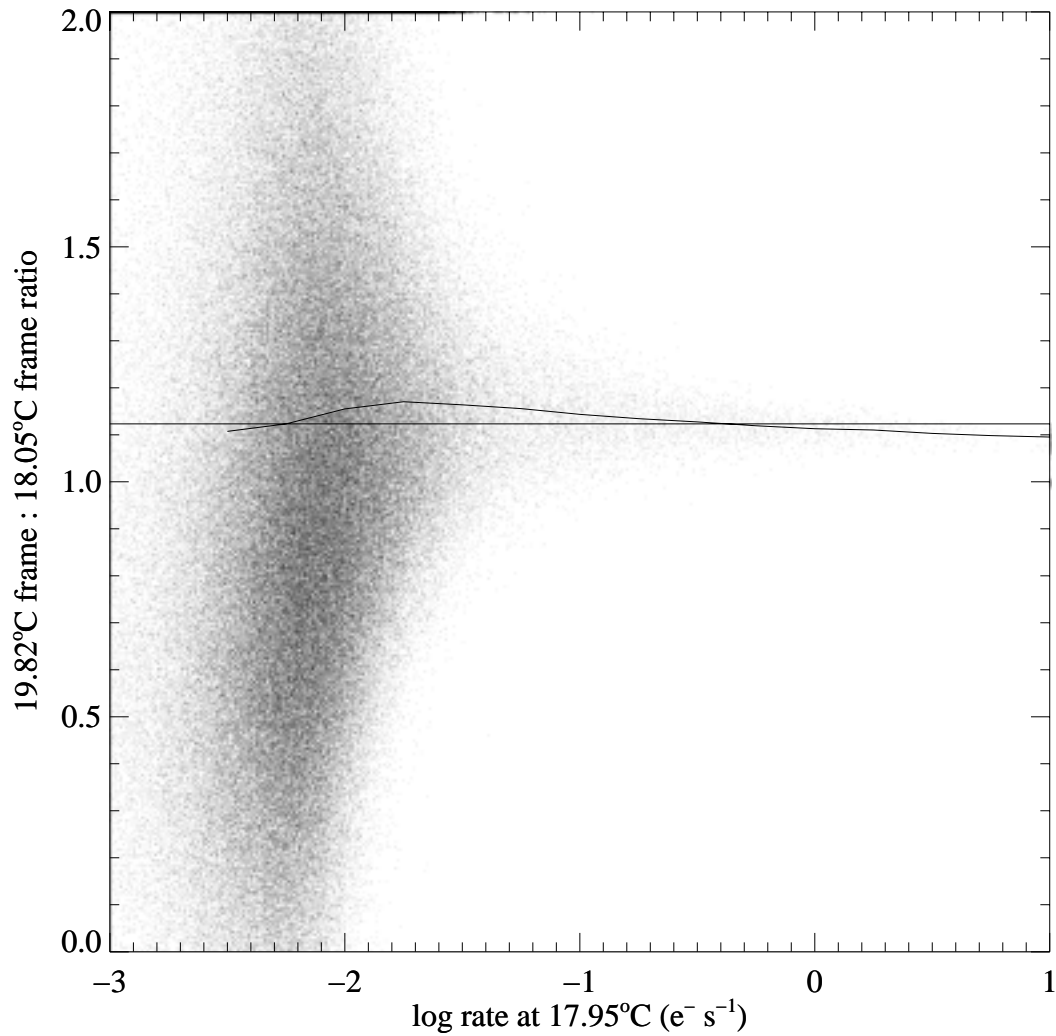


**Figure 1:** The ratio of a hot frame to a cooler reference frame, plotted against the rate in a second reference frame, for every pixel on the detector. The curve shows the median rate ratio at each rate. The horizontal line shows the median of the curve. On average, the rate in a given pixel is higher in a hot frame than in the cooler reference frame, but this increase in rate is a function of the rate itself.

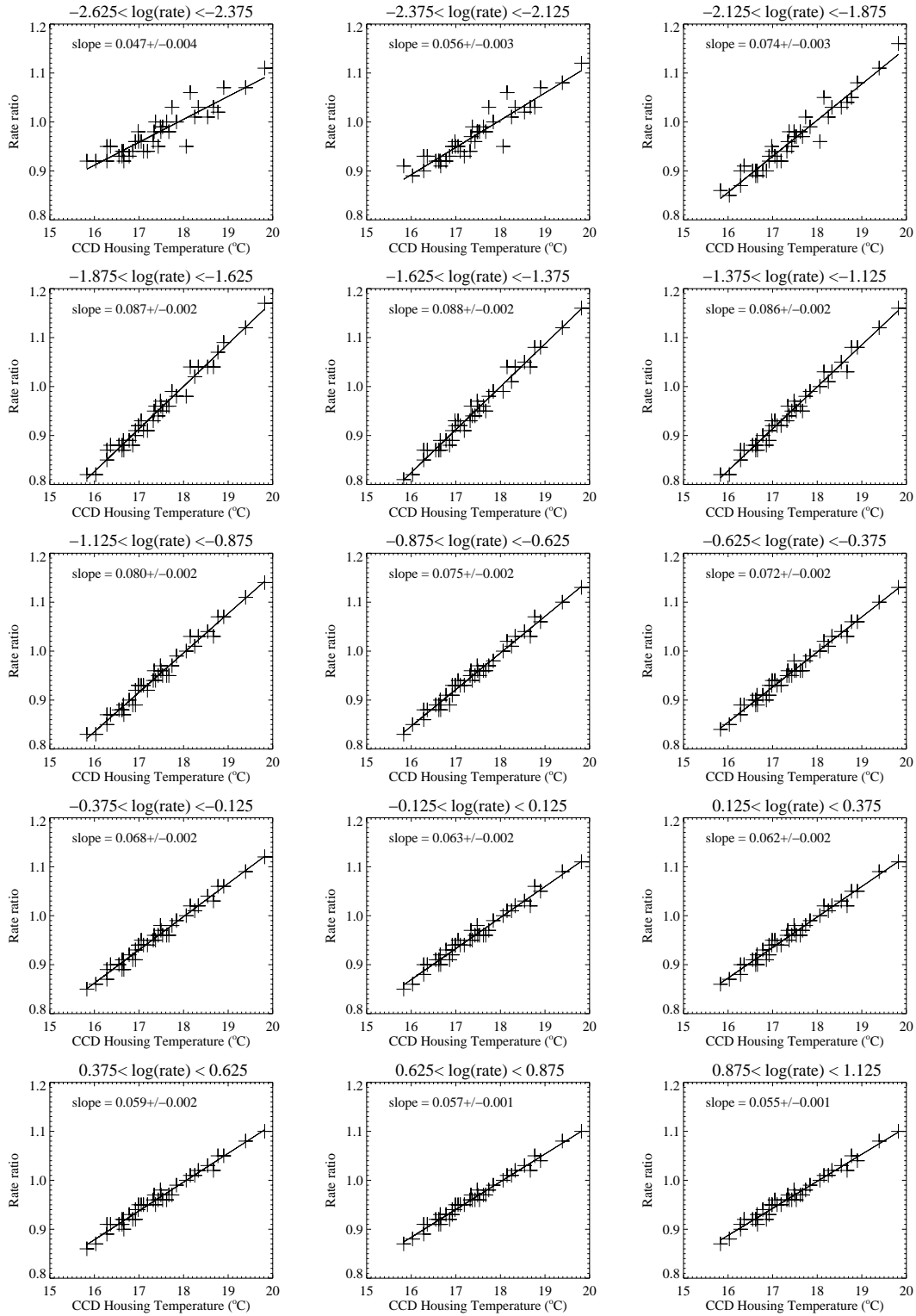


**Figure 2:** The change in rate with temperature, for pixels in a given rate range. The change in dark rate is linear, but the slope depends upon the rate in question.

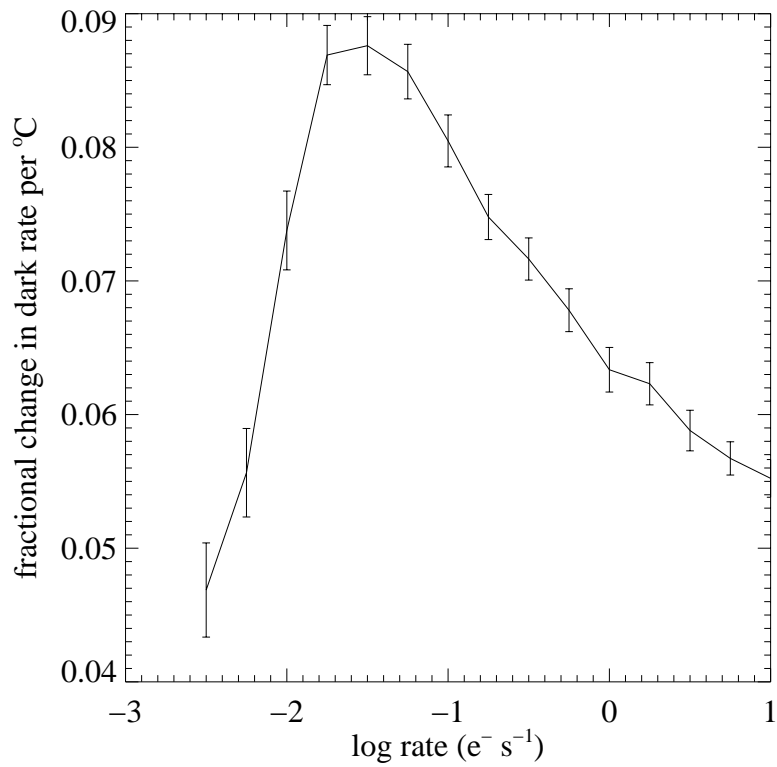


**Figure 3:** The fractional change in dark rate for every  $^{\circ}C$ , as a function of dark rate. This is simply a plot of the slopes in Figure 2. Pixels with low dark rates will increase in rate by about  $5\%/^{\circ}C$ ; pixels with moderately high dark rates will increase in rate by nearly  $9\%/^{\circ}C$ ; the pixels with the highest dark rates will increase in rate by about  $6\%/^{\circ}C$ .

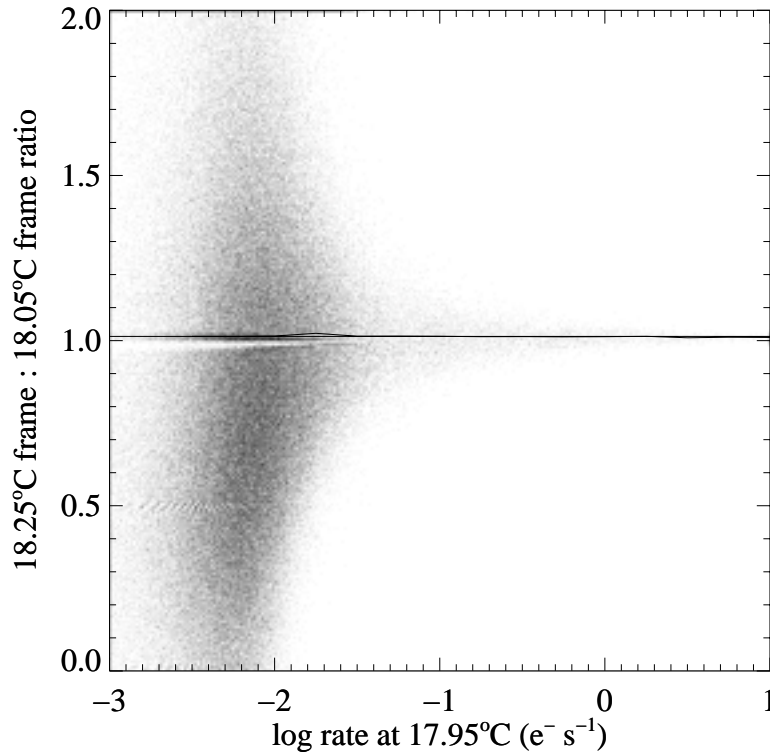


**Figure 4:** The same as Figure 1, but the hot frame has been replaced by a frame at nearly the reference temperature. Note that the median ratio is nearly unity for all rates, as expected.

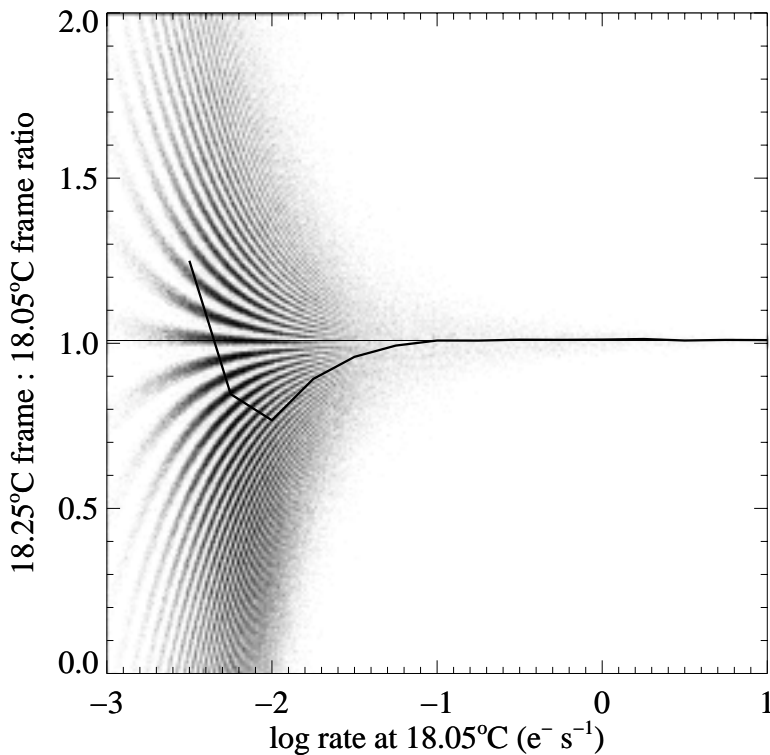


**Figure 5:** The same as Figure 4, but now the same reference frame is used (incorrectly) for the ratio on the y-axis and the rate on the x-axis. Because the abscissa and ordinate are not independent, the resulting curve is skewed, even though there should be little difference in dark rate between frames at nearly the same temperature. With only two frames, the quantization at low count rates manifests as banding in the plot.

## Conclusions

The STIS CCD dark rate during Side-2 operations depends upon the temperature of the CCD, and the strength of that temperature dependence also depends on the dark rate itself. The dark rate in individual pixels increases by approximately 5% - 9% for every °C increase in detector temperature, with the actual increase dictated by the rate. For pixels within a given range of dark rate, the increase in dark rate with temperature is very linear, showing that the CCD housing temperature is a good proxy for the detector temperature.

At this time, we have no physical explanation for why the dark rate dependence on temperature is also a function of rate. One contributing factor might be the charge transfer efficiency (CTE). Because of CTE degradation, some signal is lost when charge is transferred through the chip during readout, and the effect is exaggerated for fainter signal levels. In the dark exposures discussed herein, the pixels with the highest dark rates (e.g.,  $> 1 \text{ e}^- \text{ s}^{-1}$ ) would not be affected by the CTE degradation as much as the pixels with more modest dark rates (e.g.,  $0.03 \text{ e}^- \text{ s}^{-1}$ ). Thus, the increase in signal at increasing temperature would boost the CTE for the pixels with modest dark rates more than it would boost the CTE for the pixels with high dark rates; this could be part or all of the reason why the curve in Figure 3 decreases for rates higher than  $0.03 \text{ e}^- \text{ s}^{-1}$ . The effects of CTE do not obviously explain the behavior of this curve in the regime of very low count rates ( $< 0.03 \text{ e}^- \text{ s}^{-1}$ ), however. In any case, if the changes in the temperature dependence of the dark rate (for different rates) are primarily governed by CTE, this complicates dark subtraction. Because the CTE effects on a given pixel depend upon the signal in neighboring pixels, there will always be a limitation to the accuracy of dark subtraction in the case where hot pixels in the dark frame are more isolated than they are in the science data.

A first order dark subtraction for Side-2 CCD science data would involve the following process: first, a superdark would be created from individual dark frames, with each dark frame scaled by a constant factor depending upon the temperature (e.g., 7%/°C), to place them all at a level appropriate for one reference temperature (e.g., 18 °C). This superdark would then be rescaled (again by a constant factor) to reflect the temperature in a given science frame, prior to performing dark subtraction on that science frame. I performed preliminary testing of this procedure, by subtracting a superdark constructed and scaled in this manner from a random hot dark in the same anneal period. Compared to the use of an ordinary superdark (from a simple average for an anneal period), the temperature-dependent dark resulted in a residual background that was globally much closer to zero (by an order of magnitude). There was also a small (10%) improvement in the rms of the residual. Furthermore, blinking by eye between the results of the two methods convincingly demonstrated a modest improvement. Given this improvement, it is likely that the CALSTIS pipeline will incorporate such a procedure for dark subtraction in the near future. Users are advised to keep track of updates to the STIS pipeline, e.g., through the STIS web pages or the STScI Analysis Newsletters (STANs).

A second order correction to STIS science data, i.e., accounting for the fact that the strength of the temperature dependence depends upon the dark rate itself, would be considerably more complicated. One possibility is the following: first, a first-order superdark is created by scaling each dark frame by a constant (rate independent) scale factor depending upon the temperature, as described in the previous paragraph. The signal-to-noise in this superdark should be sufficient to determine the rate in each pixel, and, using the data in Figure 3, this rate would be used to determine a rate and temperature dependent correction for the pixels in each individual dark frame. These corrections would then be reapplied to the individual dark frames, and a new (presumably superior) superdark would be created, representing the dark rate at a reference temperature. Prior to dark subtraction from a science frame, this superdark would then be rescaled again, on a pixel-by-pixel basis, to match the science frame temperature. I also performed some preliminary testing of this procedure, and the results show little (if any) improvement over the first-order method discussed in the previous paragraph. The problem appears to be the variation in the temperature dependence for individual pixels. The median rate of pixels within a given rate range, versus temperature, has very little scatter (see Figure 2), and the function that describes the temperature-dependent changes in dark rate for different rates is also very smooth (Figure 3), but individual pixels within any given rate regime show a wide variation in their temperature-dependence. E.g., for all pixels with very elevated dark rates of  $10 \text{ e}^- \text{ s}^{-1}$ , the median change in dark rate with temperature is  $5.5\%/^{\circ}\text{C}$ , but there are pixels with this rate that vary in rate by as little as  $3\%/^{\circ}\text{C}$ , or as much as  $8\%/^{\circ}\text{C}$ , with an excellent linear fit to the change in rate versus temperature in each case.

Thus, a user who really needs the best possible dark subtraction for the hottest pixels would probably need an even more sophisticated approach than the second-order correction given above. The contemporaneous darks for a given anneal period could be examined on a pixel-by-pixel basis, to see how each pixel varied with temperature over the course of the anneal period. Of course, this could be done only for pixels with very elevated rates, in order to achieve the needed signal-to-noise. The result would be an array of temperature scaling factors, which could be used to construct the superdark and to rescale this superdark to an appropriate level for subtraction from science frames. The process would be similar to that described in the last paragraph, but instead of relying upon the data in Figure 3, the temperature dependence of the dark rate in each pixel would be determined independent of the behavior of all other pixels. Such a correction goes far beyond the requirements of most science programs (where users will simply mask or interpolate over their pixels with elevated dark rates), but it is an option for those users trying to squeeze the most information out of their CCD images. However, such users would be better off dithering their exposures, when possible, to correct pixels with elevated dark rates.

This work was assisted by useful discussion and comments from L. Dressel, P. Goudfrooij, P. Hodge, and R. Kimble.